Analysis and Optimal Design of Batch and Two-Column Continuous Chromatographic Frontal Processes for Monoclonal Antibody Purification

Ce Shi[a], Sebastian Vogg[b], Dong-Qiang Lin[a], Mattia Sponchioni[c], Massimo Morbidelli[d]*

a. Key Laboratory of Biomass Chemical Engineering of Ministry of Education, College of Chemical and Biological Engineering, Zhejiang University, Hangzhou 310027, China

b. YMC ChromaCon, Technoparkstrasse 1, 8005 Zürich, Switzerland

c. Department of Chemistry, Materials and Chemical Engineering "Giulio Natta", Politecnico di Milano, Via Mancinelli 7, 20131 Milano, Italy

d. Institute for Chemical and Bioengineering, Department of Chemistry and Applied Biosciences, ETH 11 Zurich, Vladimir-Prelog-Weg 1-5/10, 8093 Zürich, Switzerland

Corresponding authors: Mattia Sponchioni, e-mail: mattia.sponchioni@polimi.it

Massimo Morbidelli, e-mail: massimo.morbidelli@chem.ethz.ch

Abstract

The increasing demand for efficient and robust processes in the purification of monoclonal antibodies (mAbs) has recently brought frontal chromatography to the forefront. Applied during the polishing step, it enables the removal of high molecular weight aggregates from the target product, achieving high purities. Typically, this process is operated in batch using a single column, which makes it intrinsically subjected to a purity-yield tradeoff. This means that high purities can only be achieved at the cost of lowering the product yield and vice versa. Recently, a two-column continuous implementation of frontal chromatography, referred to as Flow2, was developed (Vogg et al., *J. Chrom. A*, 1619, 460943, 2020). Despite being able of alleviating the purity-yield tradeoff typical of batch operations, the increase in the number of process parameters complicates its optimal design, with the risk of not exploiting its full potential. In this work, we developed an *ad hoc* design procedure suitable for the optimization of both batch frontal chromatography and Flow2 in terms of purity, yield and productivity. This procedure provided similar results as a multi-objective optimization based on genetic algorithm but with lower computational effort. Then, batch and Flow2 operated at their optimal conditions were compared. Besides showing a more favorable Pareto Front of yield and productivity at a specified purity, the Flow2 process demonstrated improved robustness compared to the batch process with respect to modifications in the loading linear velocity, washing buffer ionic strength and loading time, thus providing an appealing operation for integrated processes.

1. Introduction

The increasing market share of monoclonal antibodies (mAbs), with 10% annual growth and more than 70 formulations approved in the last decade, makes mAbs one of the most important classes of biopharmaceuticals today. The increasing number of therapeutic indications and the emergence of biosimilars contribute to strengthen the demand for safe, efficient and cost effective manufacturing processes(Farid et al.,2005). Continuous integrated bioprocessing indeed goes in this direction(Feidl et al.,2020;Karst et al.,2018;Vogg et al.,2018) and it is therefore encouraged by regulatory authorities(Administration,2019).

Frontal chromatography has seen increased interest for protein purification, in particular as a polishing step in the downstream processing of therapeutic proteins. Particularly relevant is its application in the purification of mAbs from high molecular weight impurities, e.g., aggregates, using cation exchange resins(Carta & Jungbauer,2020;Ichihara et al.,2018;Liu et al.,2011;Pfister et al.,2018;Stone et al.,2019a). The schematic diagram of frontal chromatography operated on a single (batch) column is shown in Figure 1a. Here, the eluate from the capture step (feed), containing both the monomer and the aggregates, is first loaded into the column. The impurity (aggregates) binds stronger to the cation exchange resin and displaces the weakly bound product (monomer), which therefore elutes first and is collected in the product pool. Since after reaching its binding capacity the impurity starts breaking through the column thus lowering the purity of the product pool, the loading phase is

continued until reaching, in general, sufficiently high purity in the pool and relatively high recovery (yield). Next, a washing step is applied to recover the residual monomer still present in the column, in order to increase further the yield, but being careful not to elute also the aggregates, which would spoil the purity below specifications. Finally, regeneration and re-equilibration (R.R.) are carried out to elute all the impurities (and remaining product) into the waste and prepare the column for the next loading step. The application of frontal chromatography in the separation of mAb aggregates from the monomer was proved advantageous in terms of product purity and yield as well as high resin utilization(Brown et al.,2010;Khanal et al.,2021;Reck et al.,2017).

In such a batch operation, the selection of the loading time and linear velocity have is crucial to process the largest amount of material, without letting too much aggregate into the product pool, thus preserving the purity. In the following washing step, the linear velocity and duration should be carefully chosen to elute as much remaining product as possible, thus maximizing the yield, while not desorbing the impurity beyond the purity specification. Extensive research activity was devoted to the improvement of the performances of frontal chromatography conducted in batch, either by modifying the resin properties(Stone et al.,2019b;Tao et al.,2012) or optimizing the operating conditions for both loading and washing(Brown et al.,2010). However, this discontinuous operation suffers from an intrinsic purity-yield tradeoff. In fact, a high monomer yield can be achieved through high loadings and harsh washing conditions, which enable the recovery of much of the product. However, these severe conditions lead also to the elution of part of the impurity, thus reducing the overall purity. On the

other hand, low loadings and too mild washing conditions enable high purity of the pool but prevent full recovery of the product, at the expense of the process yield.

In order to alleviate this purity-yield tradeoff, a novel cyclic two column continuous chromatographic process (referred to as Flow2) has been developed(Vogg et al.,2020). The schematic diagram is illustrated in Figure 1b. This is a periodic process, where each cycle is composed by two symmetrical switches, with the columns changing from upstream to downstream position moving from the first to the second switch. In turn, each switch comprises three steps. In the first one, the two columns are fed while being interconnected, so that the breakthrough of the aggregates from the first column is captured by the second one. In the following interconnected washing step, with inline dilution between the two columns, both the product and the unbound impurity left in the first column are eluted into the second column. The design of a proper inline dilution is of great importance for the success of the process. In fact, this is required to lower the ionic strength of the eluting buffer, thus providing an adsorption-favored solution for both aggregates and monomer to be captured by the second column. Finally, in the third step, the two columns are disconnected. The first one undergoes the R.R. process while the second one is loaded with the fresh feed.

With two columns interconnected during loading and the following washing with inline dilution, aggregates are prevented from eluting from the second column into the product pool and more monomer can be eluted from the first column, thus improving the tradeoff between purity and yield. In addition, the washing conditions (buffer and duration) do not need to be carefully designed as in the case of the batch operation, thus

111 increasing the process robustness. However, the design of this cyclic process needs to
112 account for the increased number of operational parameters and complexity of the
113 process dynamics, which can be best achieved using model-based
114 approaches(Andersson et al.,2014;Baur et al.,2016;Ferreira et al.,2007;Müller-Späth et
115 al.,2011;Shi et al.,2020).

116 In this work, the fundamental aspects of batch and continuous frontal
117 chromatography are analyzed. A model-based optimal design procedure, valid for both
118 batch and Flow2 processes, is developed with reference to three process performance
119 parameters: yield (recovery), purity and productivity. In particular, Pareto Fronts of
120 productivity and yield, with purity fixed at given specification values (P_{spec}), computed
121 based on reliable chromatographic models of the two processes, are discussed. Next,
122 the two processes, each operated at its own optimal conditions, are compared. This
123 analysis is conducted with reference to the polishing of a mAb of industrial relevance
124 and accounts, in addition to yield, purity and productivity(Pirrung & Ottens,2017), also
125 for the important concept of process robustness, which is a major concern particularly
126 in biopharmaceutical applications(Müller Späth et al.,2010;Siitonen et al.,2015). This
127 has been quantified using a rigorous model-based sensitivity analysis of the process
128 performance with respect to its operating process parameters.
129

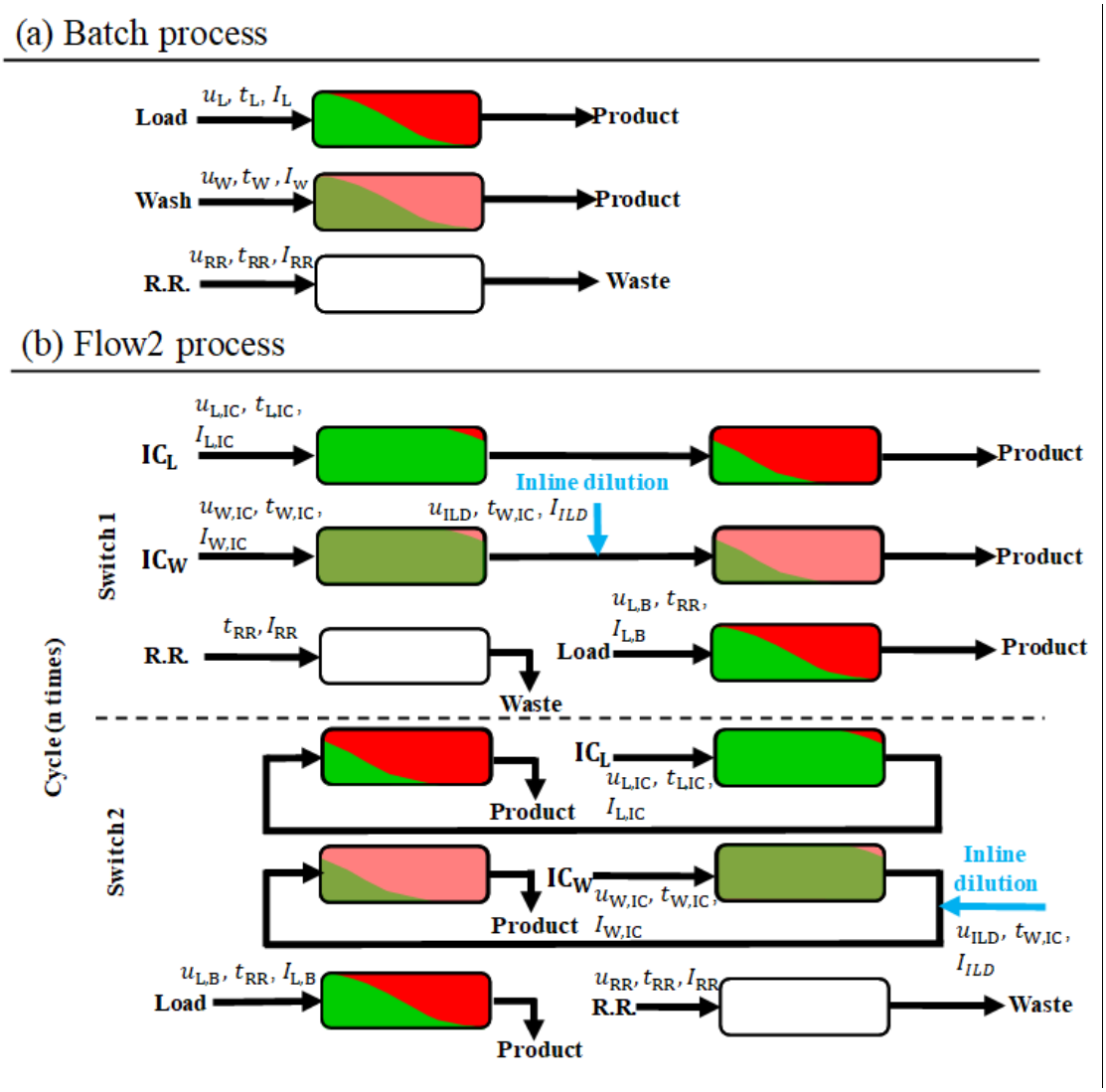

Figure 1. Schematic diagram of: (a) batch frontal chromatography, and (b) continuous Flow2 processes. Monomer is shown in red, while aggregates in green.

2. Model-Based Optimal Design Methods

2.1 The Chromatographic Model

The chromatographic lumped kinetic model with linear driving force approximation has been used in all simulations(Carta & Jungbauer,2020;Guiochon et al.,2006):

$$\frac{\partial c_{\mathrm{i}}}{\partial t} = -\frac{u_{\mathrm{sf}}}{\varepsilon_{\mathrm{t,i}}}\frac{\partial c_{\mathrm{i}}}{\partial x} + \frac{u_{\mathrm{sf}}}{\varepsilon_{\mathrm{t,i}}} d_{\mathrm{ax,i}} \frac{\partial^2 c_{\mathrm{i}}}{\partial x^2} - \frac{1-\varepsilon_{\mathrm{t,i}}}{\varepsilon_{\mathrm{t,i}}}\frac{\partial q_{\mathrm{i}}}{\partial t} \quad (1)$$

$$\frac{\partial q_{\mathrm{i}}}{\partial t} = k_{\mathrm{m,i}}(q_{\mathrm{i}}^{\mathrm{eq}} - q_{\mathrm{i}}) \quad (2)$$

with i = M, A and the boundary conditions:

$$c_{\mathrm{i}}(x, t=0) = 0$$

$$c_{\mathrm{I}}(x, t=0) = I_0$$

$$c_{\mathrm{pH}}(x, t=0) = pH_0$$

$$c_{\mathrm{i}}(x, t=0) = c_{\mathrm{i,in}}(t) + d_{\mathrm{ax,i}} \frac{\partial c_{\mathrm{i}}}{\partial x}\Big|_{x=0}$$

$$\frac{\partial c_{\mathrm{i}}}{\partial x}\Big|_{x=L_{col}} = 0$$

The mixing node in the continuous process has been simulated as follows:

$$c_{\mathrm{i,in,col2}} = \frac{c_{\mathrm{i,in,col1}} u_{\mathrm{W,IC}} + c_{\mathrm{i,ILD}} u_{\mathrm{ILD}}}{u_{\mathrm{W,IC}} + u_{\mathrm{ILD}}} \quad (3)$$

The adsorption equilibrium has been described through a surrogate model, which mimics the behavior of the DLVO-derived model, based on the competitive Langmuir isotherm and appropriate empirical correlations (Guélat et al.,2016;Vogg et al.,2020) as follows:

$$q_{\mathrm{i}}^{\mathrm{eq}} = \frac{H_{\mathrm{i}} c_{\mathrm{i}}}{1 + \sum_{\mathrm{j}} \frac{H_{\mathrm{j}} c_{\mathrm{j}}}{q_{\mathrm{j}}^{\mathrm{sat}}}} \quad (4)$$

$$q_{\mathrm{i}}^{\mathrm{sat}} = a_{\mathrm{i}}^{\mathrm{sat}} pH + b_{\mathrm{i}}^{\mathrm{sat}} \quad (5)$$

$$H_{\mathrm{i}} = \alpha_{\mathrm{i}} I^{-\beta_{\mathrm{i}}} \quad (6)$$

$$\log_{10} \alpha_{\mathrm{i}} = a_{\mathrm{i}}^{\alpha} pH + b_{\mathrm{i}}^{\alpha} \quad (7)$$

$$\beta_{\mathrm{i}} = a_{\mathrm{i}}^{\beta} pH + b_{\mathrm{i}}^{\beta} \quad (8)$$

The meaning of all variables and parameters is explained in the notation section,

while the parameter values adopted in the simulations are listed in Table 1.

Table 1. Values of the chromatographic model parameters for salt, monomer and high molecular weight aggregates (HMW)(Vogg et al.,2020)

	Parameter	Unit	Salt	Monomer	HMW
d_{col}	Column diameter	cm	----------0.5----------		
L_{col}	Bed height	cm	----------5----------		
ε_b	Bed porosity	-	----------0.39----------		
$\varepsilon_{t,i}$	(Accessible) total porosity	-	0.95	0.65	0.65
$\varepsilon_{p,i}$	(Accessible) particle porosity	-	0.93	0.43	0.43
a_i^{Sat}	Slope of q_i^{Sat} vs. pH	-	n/a	0	0
b_i^{Sat}	Intercept of q_i^{Sat} vs. pH	-	n/a	212	106
a_i^{α}	Slope of $\log_{10}\alpha$ vs. pH	-	n/a	-1.270	-3.090
b_i^{α}	Intercept of $\log_{10}\alpha$ vs. pH	-	n/a	31.22	46.90
a_i^{β}	Slope of β vs. pH	-	n/a	1.128	0.676
b_i^{β}	Intercept of β vs. pH	-	n/a	5.227	9.870
$d_{ax,i}$	Axial dispersion coefficient	cm	0.034	37	98
$k_{m,i}$	Mass transfer coefficient	1/min	170	1.3	0.53

2.2 Process performance parameters

As mentioned above, the process performance is quantified in the following using three process performance parameters, namely productivity, yield and purity. The

productivity, Pr of the target species, i.e., mAb, is defined as:

$$Pr = \frac{m}{n_{col} V_{col} t_C} \tag{9}$$

where m is the mass of target specie recovered in the product pool in one cycle of duration t_C using n_{col} columns, each with volume V_{col}. The yield, Y of the target protein is defined as:

$$Y = \frac{m}{m_{load}} \tag{10}$$

where m_{load} is the amount of target protein loaded on the column in one cycle. The purity, P is defined as:

$$P = \frac{m}{\sum_i m_i} \tag{11}$$

where the sum at the denominator is extended to the mass m_i of all proteins present in the product pool.

The buffer consumption, defined as the volume of buffer required to produce the unit amount of product, is not considered in this discussion being natively correlated to the productivity. Since in this work, if we only consider one switch for the Flow2 process, the flow rates and column volume are almost the same for the batch and continuous operations, the buffer consumption is inversely proportional to the productivity. Therefore, the latter is sufficient to compare exhaustively the two processes.

2.3 Optimization methods

The optimal design of frontal chromatographic can be complex and computationally intensive. For this, a specific procedure has been devised, based on a

series of suitable steps, and referred to as the *design procedure* (DP) in the following. This allows to facilitate and guarantee the identification of the optimal operating conditions, for a given set of performance parameters. The obtained results are compared with the corresponding results obtained by a multi-objective optimization procedure based on Genetic Algorithms.

The general concept of the DP is based on the evaluation of the loading and washing times (see Figure 1), which describe the Pareto Front of productivity and yield at a given purity equal to the specification value, $P_{\text{spec.}}$ The regeneration and re-equilibration time, t_{RR} (Figure 1) is expected to derive from a specifically designed experimental study conducted on a single column and is therefore considered as a given value in this work. The basic idea is to first compute, all the other parameters and operating conditions being fixed, the loading times leading to purity values P_1 at the end of the first loading step ranging from 100% to P_{spec}. In the following washing step, the process purity can only decrease and the corresponding duration is computed such that, for each one of the previous P_1 values, it leads to the required purity P_{spec}. For each pair of loading and washing time values, we then compute the corresponding productivity and yield values, being in all cases the purity equal to P_{spec}. At this point, we can order all the obtained values in a productivity versus yield plot and obtain the desired Pareto Front at fixed purity. This procedure can be repeated by changing any other of the relevant parameters, like the buffer composition or the column or particle size, and compute the new Pareto Front. This approach is useful not only to find the optimal operating conditions of the process, but also to quantify the robustness of a

given process design, as well as the economic impact of the different operating conditions.

Alternatively, the optimization problem can be approached as a whole, without attempting any problem decomposition, using a fully general multi-objective optimization algorithm. The function 'Gamultiobj' of the MATLAB library, based on a Genetic Algorithm, has been used in this work and the obtained results are compared with those of the *ad-hoc* design procedure.

In the next section, we describe in detail the algorithm to compute the optimal loading and washing times described above for both the batch and the Flow2 processes.

3. Optimal Design of Frontal Chromatography Processes

3.1. The Batch Process

The Pareto Front of productivity and yield with fixed $P_{\text{spec,}}$ computed with both methods, are compared first in the case of a batch process. All parameters, unless otherwise specified, are kept constant at the values summarized in Table 2.

Table 2. Batch Operating Conditions

Parameters	Unit	Value
$c_{\text{L, mono}}$	g/L	4.5
$c_{\text{L, agg}}$	g/L	0.5
I_{L}	mM	80
I_{W}	mM	120
I_{RR}	mM	1000

pH_L	-	5
pH_W	-	5
pH_{RR}	-	5
u_{L}	cm/hr	300
u_{W}	cm/hr	300
u_{RR}	cm/hr	300
t_{RR}	min	15

For illustrative purposes, P_{spec} was set to 99%. The DP method is based on the following three steps.

Step 1: Determination of the set of loading times t_L leading to a purity P_1 at the outlet of the column in the range 100% - P_{spec} (Figure 1a).

As t_{L} increases, first the product breaks through the column into the product pool, followed by the impurity at longer times, thus reducing the purity in the product pool, P_1, as shown in Figure 2a. As the loading proceeds, the purity decreases from 100% until $P_1 = P_{\mathrm{spec}}$, which indicates the maximum acceptable value of t_{L}, $t_{\mathrm{L,max}}$. In this condition, in fact, the washing time in the next step should be set to zero to avoid any further decrease in purity below P_{spec}. Of course, this extreme situation would not allow for any improvement in the process yield. Accordingly, at optimal operation, the value of t_{L} should be shorter than 72 min, which corresponds to P_1 values ranging from 100% to the P_{spec} = 99% value.

Step 2: For each $t_L < t_{L,max}$, computation of the final Purity (P) and Yield (Y) at increasing washing time, t_W until $P=P_{spec}$ and recording of the maximum washing time,

241 $t_{W,\,P=Pspec}$.

242 The obtained process yield and purity values are shown in Figure 2b as a function
243 of the washing time, t_W, as an example for the case of t_L=60 min and P_1=99.5%. It is
244 seen that the process purity, *P* decreases while *Y* increases for increasing washing times.
245 The decrease in the process purity is because more eluate, including both product and
246 impurity, is washed out into the product pool at increasing t_W. On the other hand, the
247 yield increases when increasing t_W since more product is recovered. By selecting $P = P_{spec}$, the corresponding values of the yield, $Y_{P=Pspec}$ and the maximum washing time,
248
249 $t_{W,P=Pspec}$ are found.

250 *Step 3: Computation of Y and Pr at all* $t_L < t_{L,max}$ *and the corresponding* $t_{W,P=Pspec}$ *and*
251 *derivation of the Pareto Front at fixed purity equal to* P_{spec}.

252 Figure 2c reports the trend of $Y_{P=Pspec}$ and $Pr_{P=Pspec}$ as a function of the $t_{W,P=Pspec}$
253 corresponding to a specific process purity, P_{spec} = 99%. The process yield increases
254 with $t_{W,P=Pspec}$ since more product can be recovered when extending the duration of the
255 washing step. On the other hand, this gain in the yield comes at the expenses of a
256 reduction in the productivity, computed through equation (19), which decreases with t_W.
257 This leads to the tradeoff between *Pr* and *Y* illustrated by the Pareto Front, calculated
258 at fixed P_{spec} = 99%, shown in Figure 3.

259

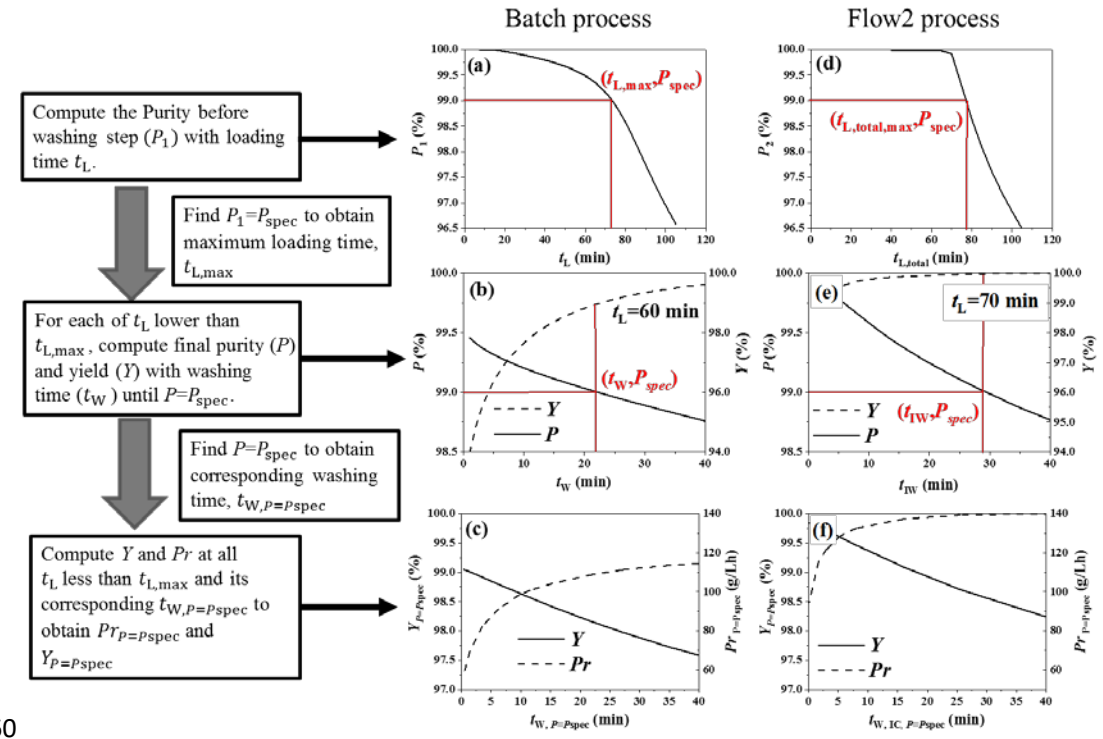

Figure 2. The design procedure for the batch and Flow2 optimization. (a) Batch P_1 as a function of the loading time; (b) Batch P and Y as a function of the washing time at t_L=60 min and P_1= 99.5% (c) The relationship between $Y_{P=Pspec}$ and $Pr_{P=Pspec}$ as a function of $t_{W,P=Pspec}$ for a batch process. (d) Flow2 P_2 as a function of the loading time, $t_{L,total}$; (e) Flow2 P and Y as a function of the washing time at $t_{L,total}$ = 70 min and P_2=99.8% (f) The relationship between $Y_{P=Pspec}$ and $Pr_{P=Pspec}$ as a function of $t_{W,P=Pspec}$ for a Flow2 process.

The results of the *ad hoc developed design procedure* (DP) are compared with those of a general multiobject Genetic Algorithm (GA), using 50 individuals per generation and a maximum of 200 generations. The purity constraint has been introduced by imposing heavy penalties on purity values smaller than P_{spec}. At each iteration, the 35 fittest individuals are selected to plot the Pareto Front and produce the

next generation. The GA optimization is terminated when the 200th generation is reached or when the average relative change in the best fitness function value, with respect to the previous generation, is less than or equal to the function tolerance (10^{-4}). The performance values corresponding to the best 35 individuals in the last generation are compared with the Pareto Front computed through the DP in Figure 3. It is seen that all the points corresponding to the GA optimization are on or slightly below the curve generated by the DP, indicating that the two methods provide essentially the same result. In addition, it is found that all the points obtained through the GA method exhibit a purity value equal to the constrain value of 99% with a maximum 1% relative deviation.

It is worth noticing that, although the two methods give equivalent results, the associated computational effort is quite different. In the *design procedure*, only 35*10 objective functions are calculated: 35 for getting the Pareto Front, and 10 each for determining the t_W values corresponding to 99% purity. On the other hand, in the multi-objects GA optimization, 50*200 functions are calculated: one for each of the 50 individuals constituting each of the 200 generations. Although fewer cases calculated make the DP method less computationally intensive, it requires a good understanding of the process and of the influence of the different process parameters over the process performance. In fact, this relationship needs to be clearly specified at each step of the process. In turn, if the process is complex enough, with a large number of parameters interactively influencing the process performance, GA is recommended for process optimization.

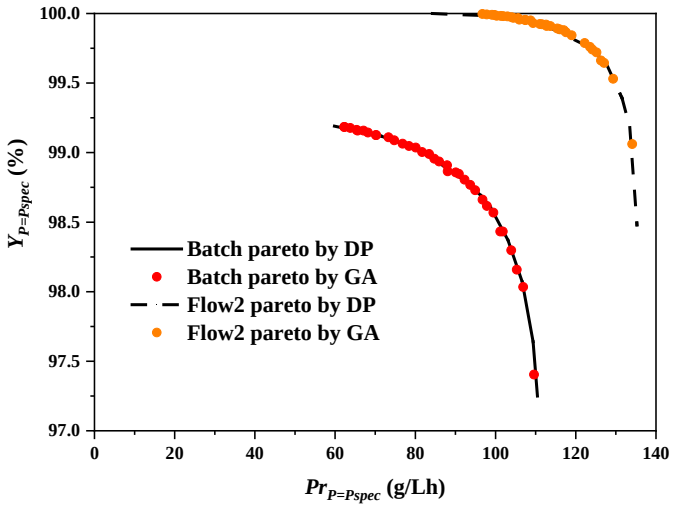

296

297 *Figure 3. Pareto Front of Pr and Y computed with the design procedure (DP)*

298 *compared with the results of the global optimization based on genetic algorithm (GA),*

299 *for P_{spec} = 99% and other parameter values as in Tables 1, 2 and 3.*

300

301 **3.2 Continuous Flow2 Process**

302 The two optimization methods considered above have been developed and

303 compared also for the Flow2 process. In particular, we optimized the interconnected

304 loading and washing times, $t_{L,IC}$ and $t_{W,IC}$ (Figure 1b) in order to obtain the Pareto Front

305 of productivity, *Pr* and *Y* with fixed purity P_{spec} = 99%. Note that in this process, the

306 batch loading time is fixed and equal to the regeneration and re-equilibration time, $t_{R.R.}$,

307 which is considered as a given constant in this analysis (Figure 1b). Accordingly, the

308 total loading time given by $t_{L,total} = t_{R.R.} + t_{L,IC}$, can actually be changed only through

309 the interconnected loading time, $t_{L,IC.}$ All remaining parameters are kept constant and

310 equal to the values summarized in Tables 1 and 3. It is to be noted that all the simulation

311 results reported for the continuous Flow2 process refer to steady state conditions. These

are obtained by simulating the entire dynamics of the process and considering the transient behavior completed when the mass flow of each protein entering and leaving differ for no more than 1.0%, which means that no protein is accumulated or lost in the system during every switch.

Table 3. Flow2 Operating Conditions

Parameters	Unit	Value
$c_{\mathrm{L,\,mono}}$	g/L	4.5
$c_{\mathrm{L,\,agg}}$	g/L	0.5
$I_{\mathrm{L,IC}}$	mM	80
$I_{\mathrm{L,B}}$	mM	80
I_{W}	mM	120
I_{ILD}	mM	10
$I_{\mathrm{R.R.}}$	mM	1000
$pH_{L,IC}$	-	5
$pH_{W,IC}$	-	5
pH_{ILD}	-	5
pH_{RR}	-	5
$u_{\mathrm{L,IC}}$	cm/hr	300
$u_{\mathrm{W,IC}}$	cm/hr	300
u_{ILD}	cm/hr	300
$u_{\mathrm{L,B}}$	cm/hr	300
$u_{\mathrm{R.R.}}$	cm/hr	300

$t_{R.R.}$	min	15

Differently from the batch process, the Flow2 process has two loading phases within one switch: interconnected and batch loading. In the following, we consider these two steps together with a total duration, $t_{L,total} = t_{R.R.} + t_{L,IC,}$ with a purity value P_2, which is analogous to the purity P_1 considered for the batch process. After the washing step, the product purity is indicated as P, which represents the final product purity at the end of the switch as indicated in Figure 1b.

The design procedure in this case is organized as follows:

Step 1: Simulation of the process for different $t_{L,total}$ leading to $P_{spec} < P_2 < 100\%$.

As shown in Figure 2d, the obtained P_2 decreased as a function of the loading time, $t_{L,total}$, starting from 100% to values below the imposed process purity specification, $P_{spec\ =\ 99\%}$, which is reached at $t_{L,total,max}$ = 78 min. This is due to the progressive breakthrough of the impurities as the loading is protracted.

Step 2: For each $t_{L,total} < t_{L,total,max}$, , computation of P and Y for the whole process at increasing interconnected washing time ($t_{W,IC}$ in Figure 1b) until $P = P_{spec}$.

Once defined the maximum loading time to avoid purity lower than $P_{spec,}$ different washing times were simulated and the corresponding P and Y determined. As an example, Figure 2e shows the results obtained for the pair of values $t_{L,total}$ = 70 min and P_2 =99.8%. As expected, it is seen that as the washing time increases, the purity decreases while the yield increases, for the same reason already discussed in the case of the batch process. The values $Y_{P=P\text{spec}}$ and $t_{W,P=P\text{spec}}$, corresponding to the requested

purity value P_{spec}, can be then obtained for each $t_{L,total}$.

Step 3: Computation of Y and Pr at each $t_{L,total} < t_{L,total,max}$ *and the corresponding* $t_{W,IC,P=Pspec}$ *and derivation of the Pareto Front at fixed purity equal to* P_{spec}.

Figure 2f represents the change of $Y_{P=Pspec}$ and $Pr_{P=Pspec}$ of Flow2 as a function of the $t_{W,ICP=Pspec}$ which leads to a specific process purity, P_{spec} = 99%, for the different loading times. The trends of $Y_{P=Pspec}$, $Pr_{P=Pspec}$ are similar to the case of the batch process. In particular, while the yield is improved due to a higher recovery of the product, the increase in the washing time leads to a decrease in the process productivity, with the typical tradeoff discussed above. This tradeoff is clearly visualized in the Pareto Front for productivity and yield at fixed purity equal to P_{spec} in Figure 3.

The latter is compared in the same figure with the corresponding Pareto Front for the batch frontal chromatography process, obtained as discussed above. The higher efficiency of the Flow2 process, which will be discussed later in more detail, is clearly indicated by the movement of the Pareto Front to the upper right corner of the figure, thus demonstrating that this continuous operations enables alleviating a recurrent tradeoff in protein purification.

As mentioned above, the multi-object global optimization of the Flow2 process has also been performed based on a genetic algorithm, using 50 individuals per generation and a maximum of 300 generations. The obtained results, corresponding to the 35 best individuals in the last generation, are shown by the points shown in Figure 3 and compared with the results of the *ad hoc* design procedure. It is seen that the two methods provide equivalent results, although the GA approach requires a significantly

larger computational effort, as already discussed in the context of the batch process.

4. Analysis and Comparison of Optimized Batch and Flow2 Process Performance

A general difficulty when comparing different processes, and not only in chromatography, is to select "fair" conditions for the comparison, that is operating conditions that do not favor one or the other. In this work, we consider each process under independently optimized operating conditions. In particular, we are going to analyze the behavior of batch and Flow2 processes as a function of operating parameters which are known to be most relevant in chromatography, such as linear velocities in the columns and composition of the loading and washing buffers. In all cases, we consider for each process the optimal Pareto yield-productivity (with fixed purity, P_{spec}) obtained by optimizing the durations of both the loading and washing steps. In the following, the design procedure developed in this work will be used, since we have shown that this provides the same results as a general multi-objective optimization, but with lower computational effort. The objective is to analyze and compare the behavior of each of such processes with respect to both process performance and robustness.

4.1 Relevant Performance Parameters

In the real industrial application of mAb manufacturing, purity values well above 95% are typically needed in polishing steps after protein capture. In Figure 4, the tradeoff between productivity and yield for optimal batch process operations at specification purities, P_{spec} equal to 95%, 98% and 99% is shown. It can be seen that

more stringent purity constraints move the Pareto Front to the lower left corner with correspondingly lower values for both productivity and yield. It can also be seen that the yield is always higher than 98%, indicating that this is not the discriminating performance parameter in designing frontal chromatography processes. Accordingly, in the following we will base the process comparison on the tradeoff between yield and productivity as well as on the operation robustness, with a stringent purity specification of P_{spec} = 99%..

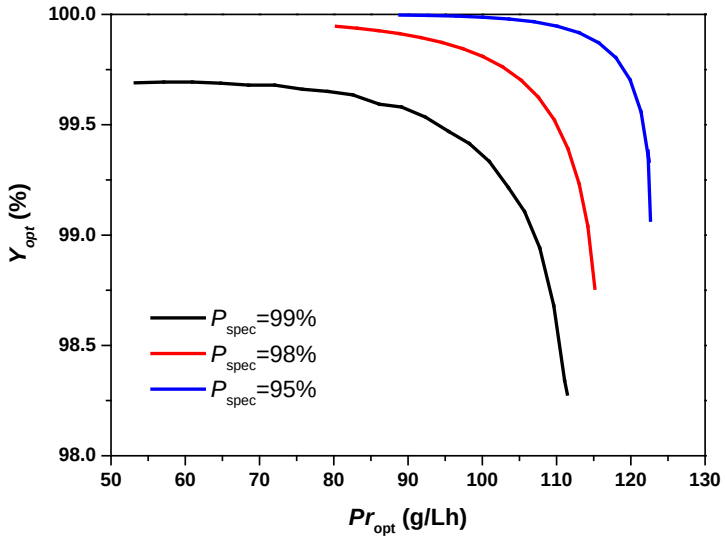

Figure 4. Tradeoff between yield and productivity (Pareto Front) for the batch process at various P_{spec} values. Operating conditions as in Tables 1 and 2.

4.2 Role of Linear Velocities in Loading and Washing

In this section, the effect of the liquid velocity during loading and washing is analyzed in both Batch and Flow2 processes. The values considered range from 300 cm/hr to the value compatible with the maximum pressure drop tolerated by the stationary phase as computed through the Blake-Kozeny equation(Abulencia &

Theodore,2009)

$$\frac{\Delta P}{L_{\mathrm{col}}} = \frac{150\mu}{d_{\mathrm{p}}^{2}} \frac{(1-\varepsilon_{\mathrm{b}})^{2}}{\varepsilon_{\mathrm{b}}^{3}} u_{\mathrm{sf}} \tag{12}$$

Considering the maximum pressure drop equal to 0.15 MPa, the maximum linear velocity of 3000 cm/hr is obtained for the 5 cm bed height and 50 μm particle radius considered in this work. The values of the remaining operating parameters used in all simulations considered in the following are listed in Tables 1 to 3.

4.2.1 Batch Process

The effect of loading and washing velocities is analyzed first with u_{L} changing from 300 to 3000 cm/hr with fixed u_{W} = 300 cm/hr, and then with u_{W} changing from 300 to 3000 cm/hr with fixed u_{L} = 300 cm/hr. The Pareto fronts obtained for various u_{L} values are shown in Figure 5a. Note that, in general, the Pareto fronts do not necessarily cover the entire range of possible yield and productivity values, since some portions of them may not be achievable with the considered operating conditions. In particular, it is seen that as the loading velocity increases, the process performance first improves, with the Pareto moving to the right of the plot, thus enabling higher productivity values for a given recovery value. This is because at higher loading velocity the loading time is shortened to the benefit of productivity. However, when further increasing the loading velocity, intraparticle mass transfer becomes more and more limiting(Farnan et al.,1997;Gotmar et al.,1999), leading eventually to the earlier breakthrough of the impurities and then to lower purity values. This explains the worsening of the Pareto front at 3000 cm/hr with respect to lower loading velocities in Figure 5a. The effect of the washing velocity is showed in Figure 5b. It is seen that as the washing velocity

increases from 300 to 900 cm/hr, the Pareto front extends to higher productivities, but it decreases again for further increasing u_W values. For the maximum allowable washing linear velocity of 3000 cm/hr, the process performance is in fact inferior to all the other washing velocities in almost the entire range of operating conditions. Limiting intraparticle mass transfer prevails at such washing linear velocity, so that more target protein remains in the column, and both yield and productivity decrease.

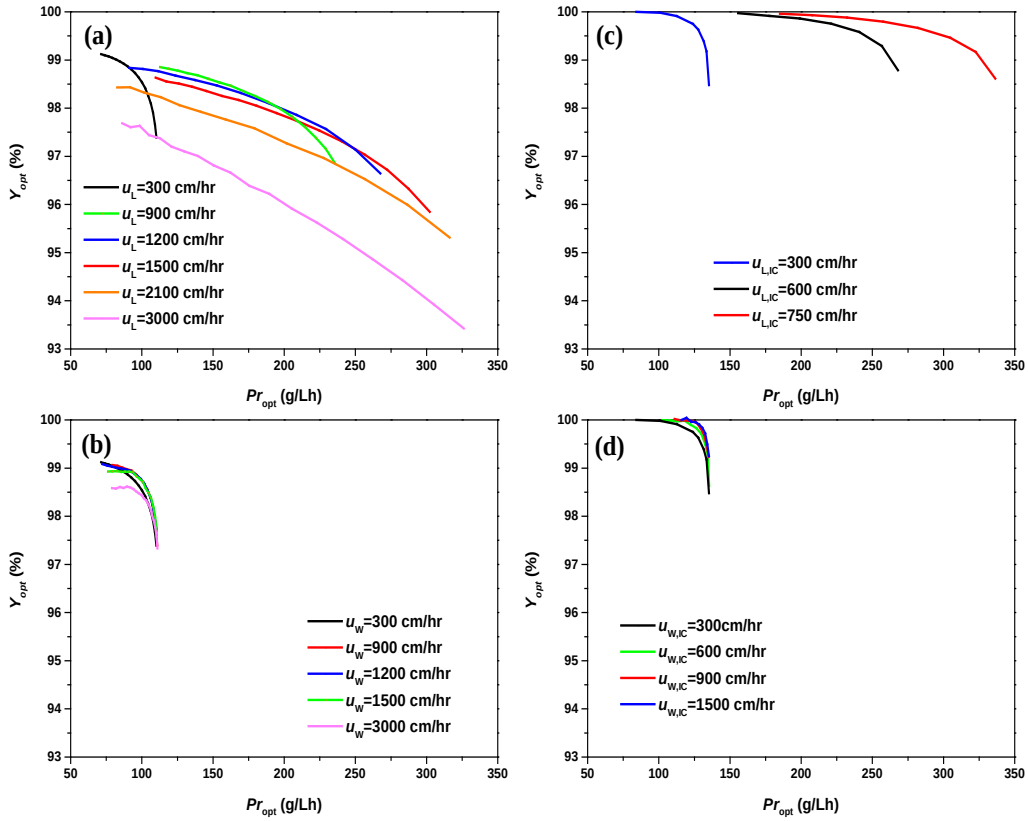

Figure 5. Tradeoff (Pareto front) between yield and productivity of (a) batch process under various loading velocities with u_W = 300 cm/hr (b) batch process under various washing velocities with u_L = 300 cm/hr (c) Flow2 process under various interconnected loading velocities with $u_{W,IC}$ = 300 cm/hr (d) Flow2 process under various interconnected washing velocities with $u_{L,IC}$ = 300 cm/hr

Thus summarizing, since the Pareto fronts in both Figures 5a and 5b tend to cross each other, the best velocity values have to be defined depending on the specific operating conditions. In particular, the idea of using the maximum possible velocity in either loading or washing, corresponding in this case to 3000 cm/hr, is not recommended.

4.2.2 Continuous Flow2 Process

The analysis of the role of liquid velocities in this case is more complex than for batch processes because we now deal with four velocities: the interconnected loading velocity, $u_{L,IC}$, the interconnected washing velocity, $u_{W,IC}$, the inline dilution velocity, u_{ILD} and the batch loading velocity, $u_{L,B}$. It appears reasonable to take equal the batch and interconnected loading velocities, i.e. $u_{L,IC} = u_{L,B,}$ so as to apply in both the same residence time. In addition, the inline dilution velocity is taken equal to the interconnected washing velocity, i.e. $u_{W,IC}=u_{ILD}$ as the resulting buffer composition for the downstream column remains constant independent of the linear velocity applied, thereby reducing the number of varied operating variables. Accordingly, in the following we analyze the effect of two velocities: $u_{L,IC}$ and $u_{W,IC}$. These will be changed independently, one at a time, in the range 300 cm/hr to 1500 cm/hr. The latter corresponds to the largest velocity compatible with the considered maximum pressure drop of 0.15 MPa, and it is half of the one considered in the case of the batch process because two columns are operated in series in the interconnected step. The simulation results are shown in Figure 5c and 5d.

In Figure 5c it is seen that larger values of the loading velocity, $u_{L,IC}$ improve significantly the tradeoff between yield and productivity of the Flow2 process. However, no Pareto Front could be calculated for loading velocities larger than 750 cm/hr, since it was not possible to achieve the requested purity of 99%. For such values of $u_{L,IC}$ (and of $u_{L,B}$), together with the fact that the batch loading time must be fixed to match the R.-R. time, too many aggregate breakthrough into the product pool. Nevertheless, it is found that, although the loading velocity is constrained by time scheduling, the Flow2 process can offer better performances than the batch operation. In particular, it can approach productivities larger than 300 g/L/h while keeping the yield in the order of 99%, which for the batch process (Figure 5a) can only be achieved by decreasing the productivity by at least three times in the order of 100 g/L/h.

Also in the case of the washing step, the process performance improves for increasing linear velocity values, $u_{W,IC}$ as shown in Figure 5d. This is because in the Flow2 process, the inline dilution allows all proteins washed out from the first column to be captured by the second column, regardless of the more or less harsh washing conditions in the first column. Better performance can be achieved compared to the batch process in terms of both yield and productivity.

Thus concluding, for the Flow2 process we can recommend the higher loading and washing velocities compatible with the pressure drop constraint, provided that the P_{spec} is obtained (750 cm/hr and 1500 cm/hr, respectively in this work). This is the main reason for the continuous process to exhibit better productivities than the corresponding batch operation, thus over compensating for the increased column volume utilized.

4.3 Role of Buffer Composition in Loading and Washing

In this section, the effect of the ionic strength of the loading and washing buffers is investigated. Also in this case, we analyze the effect of each one separately, by keeping the other fixed. In particular, we consider the ionic strengths of the loading buffer, I_L ($I_{L,IC}$ for Flow2) ranging from 40 mM to 120 mM, and for the washing buffer higher values, with I_W ($I_{W,IC}$ for Flow2) ranging from 80 mM to 200 mM. The values of the remaining operating parameters are summarized in Tables 1 to 3, and in particular the ionic strength for inline dilution buffer is kept constant at I_{ILD} = 10 mM.

4.3.1 Batch Process

The Pareto fronts computed for various values of the ionic strength of the loading buffer, I_L and at fixed ionic strength of the washing buffer, I_W equal to 120 mM, are shown in Figure 6a. It is seen that the process performance improves as I_L decreases. Lower ionic strength values, in fact, facilitate the displacement of the monomer by the aggregates by enlarging the difference of adsorptivity between aggregates and monomer. Using equations 6, 7 and 8, it can be seen that the ratio of the Henry coefficients of aggregates and monomer (H_{agg}/ H_{mono}) increases from about 40 to 600, as I_L decreases from 120 to 40 mM. Therefore, lower ionic strengths of the loading buffer can increase the monomer content and decrease the aggregate content in the product pool of the loading step. This comes of course in addition to the fact that using lower I_L typically implies also higher feed dilution and therefore lower protein concentration in the feed.

With respect to the washing conditions, a non-monotonic behavior is observed in Figure 6b: the process performance initially improves with increasing the wash buffer

ionic strength, but then deteriorates at higher values. In particular, at I_W = 140 mM the Pareto becomes minute, indicating that the specified purity value can be achieved only for a restricted range of yield and productivity values. The reason is that in the batch process, the washing buffer has to be carefully tuned in order to elute the remaining monomer inside the column without eluting also the aggregates. Too low I_w leads to too much monomer left in the column, thus decreasing yield and productivity, while too high I_w increases the aggregate leakage, thus leading to lower product purities.

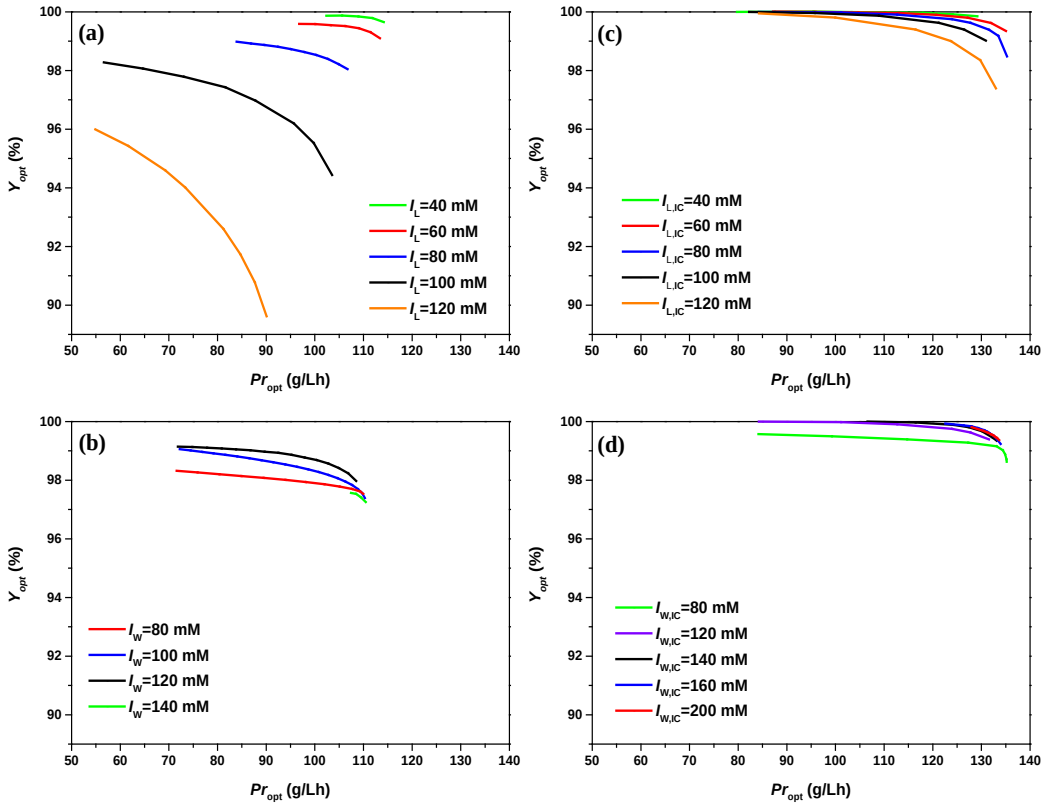

Figure 6. Tradeoff (Pareto Front) between yield and productivity of (a) Batch process for various ionic strengths of the interconnected loading buffer, I_L, with I_W = 120 mM. (b) Batch process for various ionic strengths of the interconnected washing buffer, I_W, with I_L = 80 mM. (c) Flow2 process for various ionic strengths of the interconnected

loading buffer, $I_{L,IC}$, with $I_{W,IC}$ = 120 mM. (d) Flow2 process for various ionic strengths of the interconnected washing buffer, $I_{W,IC}$, with $I_{L,IC}$ = 80 mM.

The conclusion of this analysis is that, for batch processes, while for the loading buffer lower ionic strength values (40 mM in this work) are recommended, for the washing buffer a detailed analysis is needed to identify the proper ionic strength (120 mM in this work). The latter constitutes a delicate design problem, which obviously reflects at the manufacturing level in a control problem, which may have a strong influence on the performance of the entire process. This aspect will be discussed later in terms of process robustness.

4.3.2 Continuous Flow2 Process

In the case of the Flow2 process we have four buffers involved and therefore four variables to be designed and optimized: the interconnected loading buffer ionic strength, $I_{L,IC}$, the batch loading buffer ionic strength, $I_{L,B}$, the interconnected washing buffer ionic strength, $I_{W,IC}$, and the inline dilution washing buffer ionic strength, I_{ILD}. In the following, I_B is set to be equal to I_{IC}, since, for practical reasons, it is convenient to use in both steps the same feedstock, coming from the protein A eluate and corrected to this ionic strength value. In addition, the I_{ILD} is set to be fixed at 10 mM, so that the Pareto optimization can be limited only to the interconnected loading buffer ionic strength, $I_{L,IC}$ and the interconnected washing buffer ionic strength, $I_{W,IC}$. Similarly as for the batch process, we investigate the process performance first for $I_{L,IC}$ ranging from 40 to 120 mM at fixed $I_{W,IC}$ = 120 mM, and then for $I_{W,IC}$ changing from 80 to 200 mM at

fixed $I_{L,IC}$ = 80 mM. The obtained results are shown in Figures 6c and 6d, respectively.

In Figure 6c it can be seen that, similarly to the batch process, also for the Flow2 process the performance improves, that is the Pareto Front moves to the upper right corner of the plot, as $I_{L,IC}$ decreases, although to a smaller extent. On the other hand, for $I_{W,IC}$, the data in Figure 6d show that the process performance first improves as the washing buffer ionic strength increases, but then reaches a kind of plateau for $I_{W,IC}$ values in the order of 140 to 200 mM where the process performance remains substantially unchanged. Besides providing in general better performances than the batch process, it is remarkable that this behavior of the Flow2 process is qualitatively different from that of the batch process, which indicates a superior robustness to changes in the washing buffer. In Figure 6b it can be seen, in fact, that the batch process for the largest values of $I_{W,}$ from around 100 to 140 mM, undergoes tremendous changes in its performance. This indicates that the Flow2 process can tolerate larger changes in the washing buffer ionic strength without compromising the process performance, which instead drops substantially for the batch process. This higher robustness of the Flow2 process clearly originates from the higher process flexibility, and in particular from the inline dilution. Compared to the batch process, where both the ionic strength and velocity of washing have a strong influence on process performance, the inline dilution in Flow2 expand the choice of washing conditions. In fact, washing conditions with higher ionic strength and higher velocity can be used to increase process performance, as the inline dilution allows all proteins washed out from the first column to be captured by the second column. Also, the increase in process performance can

554 improve the process robustness as it allows meeting the required product quality (i.e.
555 purity > 99%) easier compared to the variability of either batch or continuous upstream.
556 To conclude, for the Flow2 process, lower ionic strength for the loading buffer, $I_{L,IC}$
557 (40 mM in this work) and higher ionic strength for the washing buffer, $I_{W,IC}$ (higher
558 than 160 mM in this work) are generally recommended to obtain best process
559 performance in terms of both yield and productivity.
560 However, it is worth noticing that in the real industrial applications, non-aggregate
561 impurities should also be considered. With stringent washing conditions (*e.g.* high ionic
562 strength), these impurities can also be washed into the second column, and eventually
563 end up in the product pool. This phenomenon can have an impact on product quality,
564 *e.g.* in the case of proteases. However, the Flow2 process is typically carried out after
565 the capture stage, where most of such impurities are actually separated. In addition,
566 even if separation of such impurities is not achieved in Flow2, they cannot be
567 significantly enriched relative to the monomer due to the yield of almost 100%.
568
569 **5 Process Robustness and Sensitivity Analysis**
570 Robustness is an important factor when evaluating the performance of a process.
571 This is relevant at the process development stage, since higher robustness makes it
572 easier to identify operating conditions leading to optimal process performance, but it
573 matters also at the manufacturing scale, by facilitating the design of the controller
574 needed to reject possible disturbances and keep the process within specifications.
575 In this section, we address this issue through the process sensitivity

576 analysis(Varma et al.,2005). In particular, we define the normalized sensitivity, S($\psi;\varphi$)
577 of the generic output process parameter, ψ to small changes of the generic input
578 process parameter, φ as follows:

579 $$S\left(\psi;\varphi\right)=\frac{\partial\psi}{\partial\varphi}\left(\frac{\varphi}{\psi}\right) \qquad (13)$$

580 The partial derivative quantifies the local change of ψ with respect to a small change
581 of φ, *while keeping all remaining parameters constant*, and it is therefore appropriate
582 to estimate the sensitivity of the output, ψ with respect to the input, φ. The ratio φ/ψ
583 is introduced to make the sensitivity dimensionless, that is independent of the units used
584 in the evaluation of the input and output process parameters. However, it should be
585 noted that the normalized sensitivity values alone do not represent the output variability
586 due to a given input parameter, since this is also affected directly by the intrinsic
587 variability of the input parameter.

588 In the following, the sensitivity value is approximated through the incremental
589 ratio ($(\psi(\varphi+\Delta\varphi)-\psi(\varphi))/\Delta\varphi$), where the numerator represents the change in the
590 output parameter corresponding to an imposed change of the input parameter, equal to
591 +1% of the reference conditions considered in the sensitivity analysis. In particular, we
592 consider, as output process parameters, the three parameters determining the process
593 performance: productivity, yield and purity, that is ψ= *Pr*, *Y* and *P*, respectively. As
594 process input parameters we consider the loading time, the loading velocity and the
595 washing buffer ionic strength, that is φ = $t_{L,}$ u_L and I_W ($t_{L,IC}$, $u_{L,IC}$ and $I_{W,IC}$ for Flow2
596 process), respectively.

597 As reference conditions for the sensitivity analysis we select the optimized

operating conditions along the Pareto fronts with P_{spec} = 99% shown in Figure 3 for the batch and Flow2 process, respectively. Accordingly, for the various operating conditions along the Pareto Front, we compute, for each given change in the input parameter, the corresponding changes in the three performance parameters above, and from these the corresponding sensitivity values through equation (13). The obtained results, shown in Figure 7a to 7c, indicate that productivity and yield exhibit a *positive* sensitivity value, while the purity sensitivity is *negative*. This is consistent with the fact that each of the considered operating conditions belong to the Pareto front at a fixed purity value equal to 99%. The perturbed operating parameters, in fact, although leading to improvements in productivity and yield (positive sensitivity value), lead to a lower, not acceptable, purity value (negative sensitivity value) and therefore cannot be part of the Pareto Front. In the same Figure 7 it is also seen that the Flow 2 process, which can achieve larger productivity values because of its higher efficiency, also exhibits a generally better sensitivity behavior. More specifically, the very high sensitivity of the yield with respect to the washing buffer ionic strength, I_W exhibited by the batch process is largely removed in the Flow2 process.

In particular, Figure 7a shows that productivity is the most sensitive of all considered output parameters, and the corresponding sensitivity values are substantially equivalent for the two processes. Significantly lower sensitivity of the Flow2 process is observed only for the washing buffer ionic strength, $I_{W,IC}$ and for the larger productivity values. The strong reduction of the yield sensitivity with respect to I_W, mentioned above, is illustrated in Figure 7b. The sensitivity values for the Flow2

process are less than 0.015, compared to values about ten times larger, in the order of 0.1, for the batch process. This is a consequence of the stabilizing effect of the inline dilution process discussed above in the context of Figures 6b and 6d. It is worth noting that, in Figure 7b, the yield sensitivities with respect to t_L and u_L for the batch process are almost coincident. This is because these two parameters have the same effect on the loading amount, which is in fact defined by their product, (t_L* u_L), which in turns leads to the same change in the yield value. The same observation applies to the purity sensitivities, as it can be seen in Figure 7c. On the other hand, in Figure 7c, the batch process shows lower purity sensitivities than the Flow2 process, with respect to any of the input process parameters considered. However, the sensitivities with respect to the loading time and velocity are less critical in the context of process control (switching times and flow rates are typically well controlled), and the observed differences are lower than in the case above. On the other hand, the most critical sensitivity, with respect to I_W ($I_{W.IC}$), can be substantially decreased when operating at high productivity values.

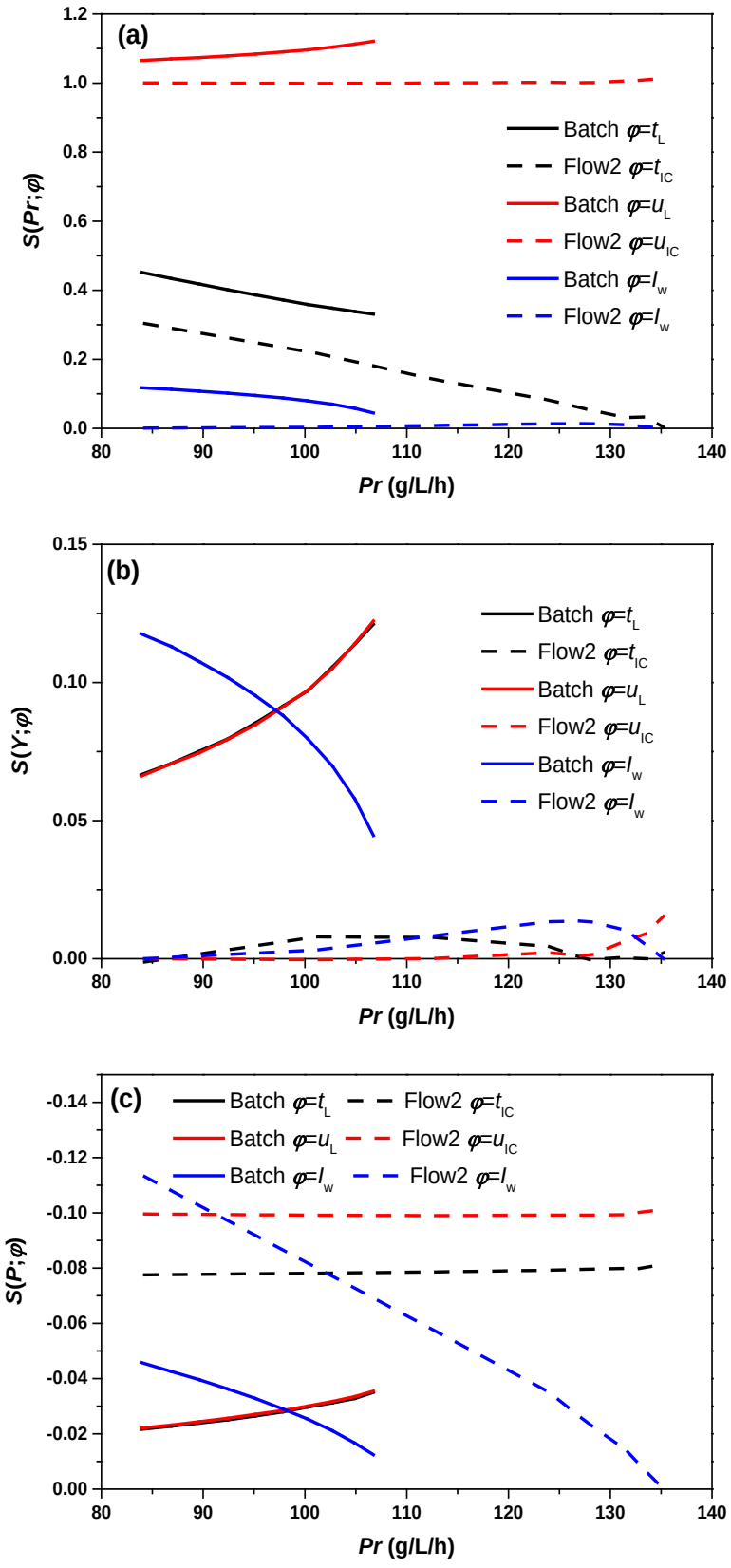

635

636 *Figure 7. Normalized sensitivity of productivity (a), yield (b) and purity (b) with respect*

637 *to $t_{L,}$ u_L and I_W for the batch process and to $t_{L,IC}$, $u_{L,IC}$ and $I_{W,IC}$ for the Flow2 process,*
638 *along the corresponding Pareto fronts shown in Figure 3.*
639
640 **6 Conclusions**
641 Frontal chromatography has been analyzed with respect to two alternative
642 implementations: a single column, batch process and a two-column, continuous process,
643 referred to as Flow2. In particular, its application in the polishing step of the processes
644 for mAb manufacturing, where the immunogenic high molecular weight species are
645 removed from the target protein, is investigated with reference to a case of industrial
646 relevance. An *ad hoc* procedure for process optimization has been developed and
647 validated through the comparison with a general multi-objective optimization
648 procedure, in terms of the Pareto Front of yield and productivity at a given purity, for
649 both processes. The derived procedure allowed a thorough comparison of the two
650 processes at their corresponding optimal operating conditions and not only in terms of
651 the performance parameters, such as yield, purity and productivity, but also with respect
652 to process robustness through a proper local sensitivity analysis.
653 The obtained results indicate that, although column interconnection puts
654 constraints on the linear velocities of the Flow2 process, this in general achieves better
655 performance in terms of both yield and productivity at a given purity, compared to the
656 batch process. An important component of this improvement is the higher flexibility
657 provided by the inline dilution process, which allows the Flow2 to better tolerate higher,
658 and therefore more advantageous, ionic strength values in the washing step. The

comparison of the normalized sensitivities computed for the two processes shows that the Flow2 process exhibits much smaller yield sensitivities than the batch one. Even more importantly, it is shown that for the Flow2 process, optimal operating conditions can be found, where the process performance is not very sensitive to the washing conditions and in particular to the buffer ionic strength. This is a very important result, since this high sensitivity represents one of the largest drawbacks of the frontal chromatography batch process, which is the reason for its lack of robustness and reflects in difficulties in determining washing conditions that can guarantee reliable operation particularly at the large scale.

The discussed robustness analysis is based on the study of the *local* sensitivity values defined by equation (13). These local values are relevant, for example, for determining the characteristics of the algorithm used to control a specific input variable, e.g. determine the largest deviations that can be allowed to the input variable. It is interesting to note that the above reached conclusion is in good agreement with the analysis reported by Vogg et al.(Vogg et al.,2020). based on a *global* definition of robustness. In particular, they compared the robustness of the two processes by considering the amplitude of the range of operating conditions, which allow respecting specific requirements in terms of process performance parameters. While their results indicate that the Flow2 process is characterized by larger robust design spaces than the batch process, our results augment this behavior by showing decreased local sensitivity of the Flow2 process towards process parameter variations at given sets of process parameters.

From all the discussion above, among the various chromatographic steps involved in the production of mAbs, frontal chromatography can be a quite promising candidate for the polishing step after protein capture with high purity, productivity and robustness.

Notations

d_p	Particle diameter (m)
$d_{ax,i}$	Axial dispersion coefficient of i component (m^2/s)
H_i	Henry coefficient ($atm*m^2/mg$)
I_{ILD}	Ionic strength of Flow2 inline dilution buffer (mM)
I_L	Ionic strength of Batch loading buffer (mM)
$I_{L,B}$	Ionic strength of Flow2 disconnected loading buffer (mM)
$I_{L,IC}$	Ionic strength of Flow2 interconnected loading buffer (mM)
I_{RR}	Ionic strength of batch and Flow2 recovery and regeneration (mM)
I_W	Ionic strength of Batch washing buffer (mM)
$I_{W,IC}$	Ionic strength of Flow2 interconnected washing buffer (mM)
$k_{m,i}$	Mass transfer coefficient of i component (m^2/s)
L_{col}	Column length (m)
Pr	Process productivity (g/Lh)
P	Product Purity
P_{spec}	Specification value for purity
u_{ILD}	Linear velocity of Flow2 inline dilution (cm/hr)
u_L	Linear velocity of batch loading (cm/hr)

$u_{L,IC}$	Linear velocity of Flow2 interconnected loading (cm/hr)
$u_{L,B}$	Linear velocity of Flow2 disconnected loading (cm/hr)
u_{RR}	Linear velocity of batch and Flow2 recovery and regeneration (cm/hr)
u_{sf}	Superficial velocity (m/s)
u_{W}	Linear velocity of batch washing (cm/hr)
$u_{W,IC}$	Linear velocity of Flow2 interconnected washing (cm/hr)
q_{i}	Concentration of i component in solid phase (mg/mL)
q_{i}^{eq}	Equilibrium concentration of i component in solid phase (mg/mL)
q_{i}^{sat}	Saturation binding capacity of i component in solid phase (mg/mL)
t_{L}	Time of batch loading (min)
$t_{L,IC}$	Time of Flow2 interconnected loading (min)
t_{RR}	Time of batch and Flow2 recovery and regeneration (min)
t_{W}	Time of batch washing (min)
$t_{W,IC}$	Time of Flow2 interconnected washing (min)
Y	Product yield
$\varepsilon_{t,i}$	Total accessible porosity of i component
μ	Mobile phase dynamic viscosity (mPas)

References

Abulencia, J. P., & Theodore, L. (2009). *Fluid flow for the practicing chemical engineer*: Wiley Online Library.

Administration, U. S. F. A. (2019). Quality considerations for continuous

manufacturing–Guidance for industry–draft guidance, from https://www.fda.gov/regulatory-information/search-fda-guidance-documents/quality-considerations-continuous-manufacturing

Andersson, N., Knutson, H., Max-Hansen, M., Borg, N., & Nilsson, B. (2014). Model-based comparison of batch and continuous preparative chromatography in the separation of rare earth elements. *Industrial & Engineering Chemistry Research*, 53(42), 16485-16493

Baur, D., Angarita, M., Müller Späth, T., & Morbidelli, M. (2016). Optimal model-based design of the twin-column CaptureSMB process improves capacity utilization and productivity in protein A affinity capture. *Biotechnology journal*, 11(1), 135-145

Brown, A., Bill, J., Tully, T., Radhamohan, A., & Dowd, C. (2010). Overloading ion-exchange membranes as a purification step for monoclonal antibodies. *Biotechnology and applied biochemistry*, 56(2), 59-70

Carta, G., & Jungbauer, A. (2020). *Protein chromatography: process development and scale-up*: John Wiley & Sons.

Ecker, D. M., Jones, S. D., & Levine, H. L. (2015*The therapeutic monoclonal antibody market*. Paper presented at the MAbs.

Farid, S. S., Washbrook, J., & Titchener Hooker, N. J. (2005). Decision-support tool for assessing biomanufacturing strategies under uncertainty: stainless steel versus disposable equipment for clinical trial material preparation. *Biotechnology progress*, 21(2), 486-497

Farnan, D., Frey, D. D., & Horvath, C. (1997). Intraparticle mass transfer in high-speed chromatography of proteins. *Biotechnology progress*, 13(4), 429-439

Feidl, F., Vogg, S., Wolf, M., Podobnik, M., Ruggeri, C., Ulmer, N.,... Butté, A. (2020). Process-wide control and automation of an integrated continuous manufacturing platform for antibodies. *Biotechnology and bioengineering*, 117(5), 1367-1380

Ferreira, S. L. C., Bruns, R. E., Da Silva, E. G. P., Dos Santos, W. N. L., Quintella, C. M., David, J. M.,... Neto, B. B. (2007). Statistical designs and response surface techniques for the optimization of chromatographic systems. *Journal of chromatography A*, 1158(1-2), 2-14

Gotmar, G., Fornstedt, T., & Guiochon, G. (1999). Peak tailing and mass transfer kinetics in linear chromatography: Dependence on the column length and the linear velocity of the mobile phase. *Journal of Chromatography A*, 831(1), 17-35

Grilo, A. L., & Mantalaris, A. (2019). The increasingly human and profitable monoclonal antibody market. *Trends in biotechnology*, 37(1), 9-16

Guélat, B., Khalaf, R., Lattuada, M., Costioli, M., & Morbidelli, M. (2016). Protein adsorption on ion exchange resins and monoclonal antibody charge variant modulation. *Journal of Chromatography A*, 1447, 82-91

Guiochon, G., Felinger, A., & Shirazi, D. G. (2006). *Fundamentals of preparative and nonlinear chromatography*: Elsevier.

Ichihara, T., Ito, T., Kurisu, Y., Galipeau, K., & Gillespie, C. (2018*Integrated flow-through purification for therapeutic monoclonal antibodies processing*. Paper presented at the MAbs.

Kaplon, H., & Reichert, J. M. (2019*Antibodies to watch in 2019*. Paper presented at the MAbs.

Karst, D. J., Steinebach, F., & Morbidelli, M. (2018). Continuous integrated manufacturing of therapeutic proteins. *Current opinion in biotechnology*, 53, 76-84

Khanal, O., Kumar, V., & Lenhoff, A. M. (2021). Displacement to separate host-cell proteins and aggregates in cation-exchange chromatography of monoclonal antibodies. *Biotechnology and Bioengineering*, 118(1), 164-174

Levine, H. L., Lilja, J. E., Stock, R., Hummel, H., & Jones, S. D. (2012). Efficient, flexible facilities for the 21st century. *BioProcess Int*, 10(11), 20-30

Liu, H. F., McCooey, B., Duarte, T., Myers, D. E., Hudson, T., Amanullah, A.,... Kelley, B. D. (2011). Exploration of overloaded cation exchange chromatography for monoclonal antibody purification. *Journal of Chromatography A*, 1218(39), 6943-6952

Müller Späth, T., Krättli, M., Aumann, L., Ströhlein, G., & Morbidelli, M. (2010). Increasing the activity of monoclonal antibody therapeutics by continuous chromatography (MCSGP). *Biotechnology and bioengineering*, 107(4), 652-662

Müller-Späth, T., Ströhlein, G., Aumann, L., Kornmann, H., Valax, P., Delegrange, L.,... Jöhnck, M. (2011). Model simulation and experimental verification of a cation-exchange IgG capture step in batch and continuous chromatography. *Journal of Chromatography A*, 1218(31), 5195-5204

Pfister, D., Nicoud, L., & Morbidelli, M. (2018). *Continuous Biopharmaceutical*

Processes: Chromatography, Bioconjugation, and Protein Stability: Cambridge University Press.

Pirrung, S. M., & Ottens, M. (2017). High-Throughput Process Development. *Preparative Chromatography for Separation of Proteins*, 269-291

Reck, J. M., Pabst, T. M., Hunter, A. K., & Carta, G. (2017). Separation of antibody monomer-dimer mixtures by frontal analysis. *Journal of Chromatography A*, 1500, 96-104

Shi, C., Gao, Z., Zhang, Q., Yao, S., Slater, N. K.,... Lin, D. (2020). Model-based process development of continuous chromatography for antibody capture: A case study with twin-column system. *Journal of Chromatography A*, 1619, 460936

Siitonen, J., Mänttäri, M., Seidel-Morgenstern, A., & Sainio, T. (2015). Robustness of steady state recycling chromatography with an integrated solvent removal unit. *Journal of Chromatography A*, 1391, 31-39

Singh, S., Tank, N. K., Dwiwedi, P., Charan, J., Kaur, R., Sidhu, P.,... Chugh, V. K. (2018). Monoclonal antibodies: a review. *Current clinical pharmacology*, 13(2), 85-99

Stone, M. T., Cotoni, K. A., & Stoner, J. L. (2019a). Cation exchange frontal chromatography for the removal of monoclonal antibody aggregates. *Journal of Chromatography A*, 1599, 152-160

Stone, M. T., Cotoni, K. A., & Stoner, J. L. (2019b). Cation exchange frontal chromatography for the removal of monoclonal antibody aggregates. *Journal of Chromatography A*, 1599, 152-160

780 Tao, Y., Chen, N., Carta, G., Ferreira, G., & Robbins, D. (2012). Modeling
781 multicomponent adsorption of monoclonal antibody charge variants in cation
782 exchange columns. *AIChE Journal*, 58(8), 2503-2511. doi:
783 https://doi.org/10.1002/aic.13718
784 Varma, A., Morbidelli, M., & Wu, H. (2005). *Parametric sensitivity in chemical*
785 *systems*: Cambridge University Press.
786 Vogg, S., Müller-Späth, T., & Morbidelli, M. (2018). Current status and future
787 challenges in continuous biochromatography. *Current opinion in chemical*
788 *engineering*, 22, 138-144
789 Vogg, S., Müller-Späth, T., & Morbidelli, M. (2020). Design space and robustness
790 analysis of batch and counter-current frontal chromatography processes for the
791 removal of antibody aggregates. *Journal of Chromatography A*, 1619, 460943
792